

Multimodal analysis of the Preferred Retinal Location and the Transition Zone in patients with Stargardt Disease

Tommaso Verdina¹  · Vivienne C. Greenstein² · Andrea Sodi³ · Stephen H. Tsang^{2,4} · Tomas R. Burke² · Ilaria Passerini⁵ · Rando Allikmets^{2,4} · Gianni Virgili³ · Gian Maria Cavallini¹ · Stanislao Rizzo³

Received: 1 September 2016 / Revised: 29 December 2016 / Accepted: 13 March 2017
© Springer-Verlag Berlin Heidelberg 2017

Abstract

Purpose The purpose of our study was to investigate morpho-functional features of the preferred retinal location (PRL) and the transition zone (TZ) in a series of patients with recessive Stargardt disease (STGD1).

Methods Fifty-two STGD1 patients with at least one *ABCA4* mutation, atrophy of the central macula (MA) and an eccentric PRL were recruited for the study. Microperimetry, fundus autofluorescence (FAF), spectral-domain optical coherence tomography (SD-OCT) were performed. The location and stability of the PRL along with the associated FAF pattern and visual sensitivities were determined and compared to the underlying retinal structure.

Results The mean visual sensitivity of the PRLs for the 52 eyes was 10.76 +/- 3.70 dB. For the majority of eyes, PRLs were associated with intact ellipsoid zone (EZ) bands and

qualitatively normal FAF patterns. In 17 eyes (32.7%) the eccentric PRL was located at the edge of the MA. In 35 eyes (67.3%) it was located at varying distances from the border of the MA with a TZ between the PRL and the MA. The TZ was associated with decreased sensitivity values (5.92 +/- 4.69 dB) compared to PRLs ($p < 0.05$), with absence/disruption of the EZ band and abnormal FAF patterns (hyper or hypo-autofluorescence).

Conclusions In STGD1 eccentric PRLs are located away from the border of MA and associated with intact EZ bands and normal FAF. The TZ is characterized by structural and functional abnormalities. The results of multimodal imaging of the PRL and TZ suggest a possible sequence of retinal and functional changes with disease progression that may help in the planning of future therapies; RPE dysfunction appears to be the primary event leading to photoreceptor degeneration and then to RPE loss.

Keywords Fundus autofluorescence · Fundus flavimaculatus · Eccentric fixation · Microperimetry · Preferred retinal location · SD-OCT · Stargardt disease

✉ Tommaso Verdina
tommaso.verdina@gmail.com

¹ Institute of Ophthalmology, University of Modena and Reggio Emilia, Via del Pozzo 71, 41100 Modena, Italy

² Department of Ophthalmology, Columbia University, New York, NY, USA

³ Department of Translational Surgery and Medicine, Eye Clinic, University of Florence, Largo Brambilla 3, Florence 50134, Italy

⁴ Barbara & Donald Jonas Stem Cell & Regenerative Medicine Laboratory, and Bernard & Shirlee Brown Glaucoma Laboratory, Departments of Ophthalmology, Pathology & Cell Biology, Institute of Human Nutrition, College of Physicians and Surgeons, Columbia University, New York, NY 10032, USA

⁵ Department of Genetic Diagnostics, Azienda Ospedaliero Universitaria Careggi, Florence, Italy

Introduction

Stargardt disease is a common form of juvenile macular degeneration characterized by the presence of progressive loss of central visual function [1–4]. It is generally an autosomal recessive disorder with mutations in the *ABCA4* gene. This gene codes for an ATP-binding cassette located in the photoreceptor outer segment and its impairment causes an abnormal degradation of visual cycle by-products leading to a diffuse accumulation of metabolites (lipofuscin, bisretinoids) within retinal pigment epithelium (RPE) with consequent RPE and photoreceptor degeneration [5–7].

Atrophy at the posterior pole is characteristic of advanced stages of STGD1 and, with increased disease severity and/or disease duration, this can extend beyond the central macula. Due to this macular atrophy (MA), STGD1 patients develop eccentric and unstable fixation; they adopt a preferred retinal locus (PRL) located in a relatively spared area of the retina [8–12].

The existence of the non-foveal or eccentric PRLs in STGD1 has been known for many years, but the exact sequence of the retinal degenerative processes contributing to its development and location still remains unclear [13, 14]. Patients with age-related macular disease (AMD) usually develop an eccentric PRL that is typically located at the edge of the MA in an area of relatively healthy retina [15] and some authors hypothesize that different cortical adaptation mechanisms may be active in AMD and juvenile forms of macular degeneration [11]. In STGD1, the eccentric PRL is often located some distance from the superior edge or border of the area of atrophy [10] and the existence of a TZ, between healthy and severely affected retina, has been described [16].

The purpose of this study was to use multimodal imaging techniques, SD-OCT, SW-FAF and microperimetry to evaluate the PRL and the TZ in a group of patients with STGD1. A comparison of the results of these functional and structural tests should improve our understanding of the rationale behind the choice of the PRL for fixation in STGD1 patients and provide insight into the mechanism of disease progression.

Methods

Patients diagnosed with STGD1, BCVA \geq 20/400 in the better eye, with a central macular atrophic area (MA) and an eccentric PRL were recruited at the Eye Clinic of Florence (Italy) and at the Edward S. Harkness Eye Institute of Columbia Medical Center in New York City (NY).

The medical records and results of imaging studies of 52 eyes of 52 consecutive patients were retrospectively reviewed according to the guidelines of the local Ethical Committees at the Florence Hospital and Columbia University. For each patient the eye with more stable fixation was selected for analysis. All procedures were in accordance with ethical standards of the institutional and/or national research committee and with the 1964 Helsinki Declaration and its later amendments or comparable ethical standards. For this type of study, formal consent was not required.

Criteria for the STGD1 phenotype included the following: appearance of the disease in the first or second decade of life; bilateral progressive central vision loss; macular atrophy/dystrophy; normal caliber of retinal vessels; and absence of pigmented bone spicules.

Fifty patients carried two *ABCA4* pathogenic mutations; in two patients only one *ABCA4* pathogenic mutation was detected.

At the time of their examination, all tested eyes of patients were found to be phenotypically categorized as either stage 1 (19 eyes, 36.5%), 2 (ten eyes, 19.2%), 3 (15 eyes, 28.9%) or 4 (eight eyes, 15.4%) of the clinical disease spectrum of STGD1 as defined by Fishman et al. [17].

Patients were excluded from the study if they had refractive errors exceeding \pm 5D, significant cataract, other ocular diseases, and were $>$ 69 years of age. In addition none of the study patients had a family history of other inherited retinal or systemic disorders. All patients underwent a complete ophthalmic examination with BCVA determination, color fundus photography, microperimetry, FAF and SD-OCT.

Microperimetry was performed with the MP-1 (Nidek Technologies, Padova, Italy) following pupil dilation (0.5% tropicamide and 2.5% phenylephrine) and 20 minutes of adaptation to dim room illumination). A 10-2 pattern with 68 locations was used to determine visual sensitivity in the central macular area. “white” test lights (stimulus size Goldmann III, 200 ms in duration) were presented on a dim “white” background (1.27 cd/m²) using a 4-2 procedure. The patient was asked to maintain fixation on a 2° red fixation cross during the test. The non-tested eye was occluded. Fixation stability was quantified in terms of the bivariate contour ellipse area (BCEA) as previously described [18]. We recorded the BCEAs encompassing 68.2% (BCEA68) and 99% (BCEA99) of fixation points. We defined the PRL with reference to the fovea as superior (from 45°–135° superior) nasal (from 315°–45°), temporal (135°–225°) or inferior (225°–315°). PRL location was expressed in degrees from the estimated foveal position defined by specific vascular landmarks on retinography. The distance in degrees was calculated based on the known distance between each test location on the MP-1 sensitivity map. We defined PRL “at the edge of MA” if the PRL was located $<$ 1° from the MA and as “away from the edge of MA” if the PRL was located $>$ 1° from the MA.

Visual sensitivity in the PRL was defined as the average of the sensitivity values of all the test locations included within the BCEA68. The TZ was defined as the retinal area located between the inferior boundary of the BCEA68 ellipse and the upper boundary of the dark lesion identified by FAF (see Fig. 1 and Fig. 2). Visual sensitivity in the TZ was obtained by calculating the average sensitivity of all the MP-1 test points located in that area.

FAF imaging was performed with a confocal scanning laser ophthalmoscope (Heidelberg Retina Angiograph 2 or Spectralis HRA+OCT; Heidelberg Engineering, Dossenheim, Germany) using a 30° field of view at a resolution of 1536 x 1536 pixels. An optically pumped solid-state laser (488 nm) was used for excitation and a 495 nm barrier filter was used to modulate the blue argon excitation light. Standard procedure was followed for the acquisition of FAF images, including focus of the retinal image in the infrared reflection mode at 820 nm, sensitivity adjustment at 488 nm, and acquisition of nine single 30° x

Fig. 1 Examples of PRLs - distance from the fovea

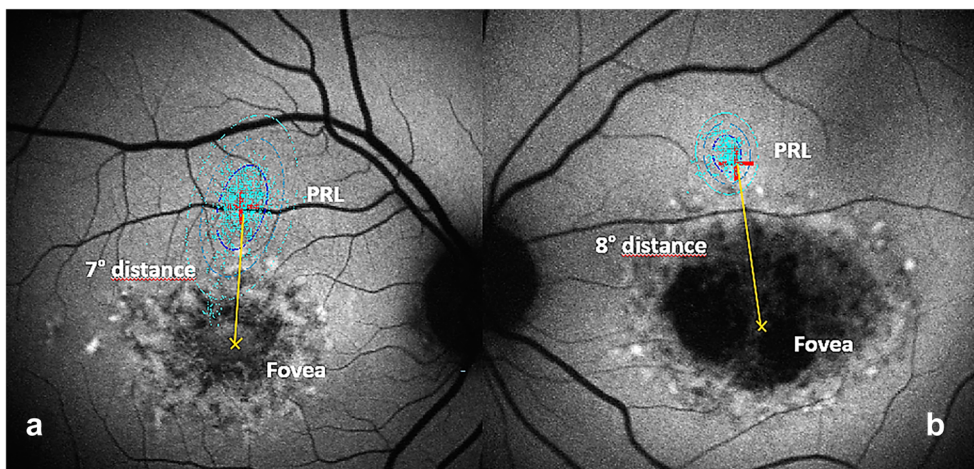
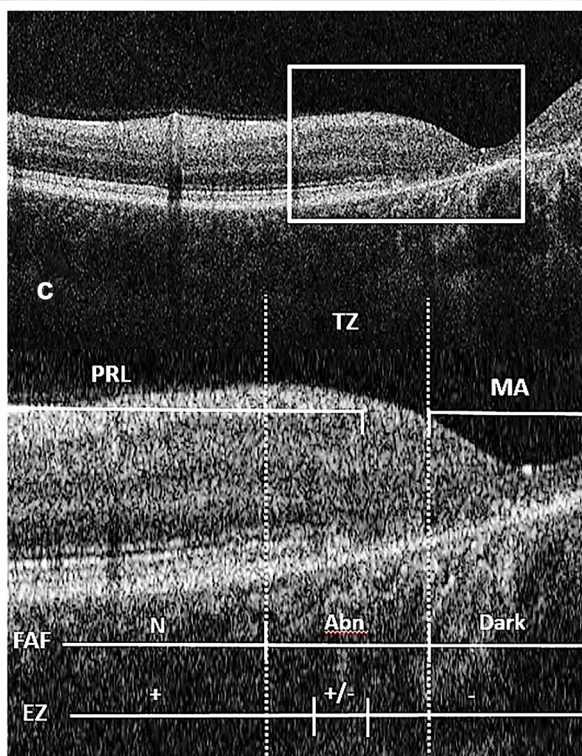
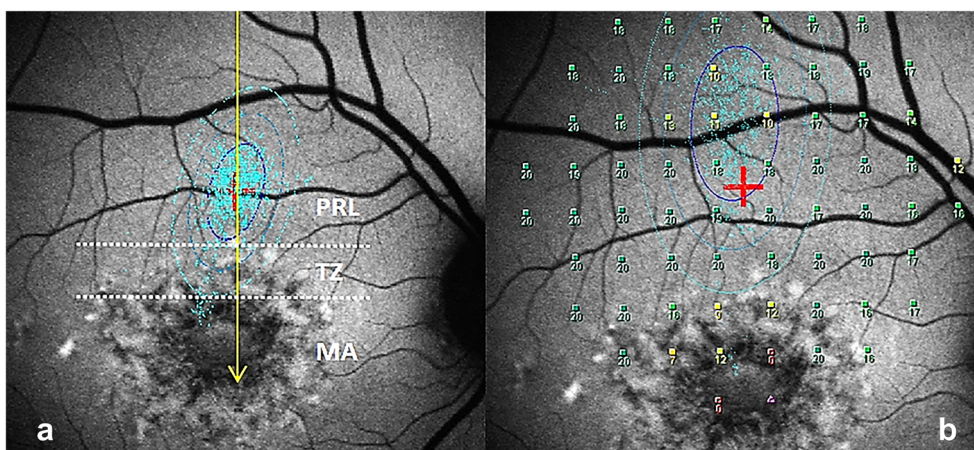


Fig. 2 Patient n.34. **a)** FAF image with fixation (BCEA), the yellow line indicates the OCT scan, the downward pointing arrow indicates the direction of the OCT scan. **b)** FAF with superimposed microperimetry results **c)** SD-OCT scan. The lower panel is at a higher magnification and shows the different areas at the border of MA. TZ= transition zone; EZ= ellipsoid zone band: (+) presence, (+/-) disruption, (-) absence.



30°. The nine single images were computationally averaged to produce a single frame with improved signal-to-noise ratio. Three FAF patterns were identified: N=normal; ABN= heterogeneous pattern of hypo/hyper autofluorescence with or without definite flecks; DARK= RPE atrophy. FAF imaging was always performed after microperimetry to avoid the possible effect of light adaptation on measures of visual sensitivity. The 30° FAF images were imported into the NAVIS software in the MP-1 system and overlaid on the MP-1 results using retinal vessel bifurcation as registration landmarks. FAF in the PRL region was assessed by analyzing the FAF pattern within the ellipse area of the BCEA68. In the TZ, it was assessed by analyzing the pattern located between the inferior boundary of the BCEA68 and the adjacent border of MA.

SD-OCT was performed in all patients in the retinal areas evaluated with the MP-1. Spectralis HRA+OCT (Heidelberg Engineering GmbH, Germany) was used in 16 patients at Columbia University and Topcon 3D-OCT 1000 (Topcon Inc., Paramus, New Jersey, USA) in 36 patients at Florence Eye Clinic. Both instruments allow for simultaneous OCT scans and fundus photograph and subsequent image superimposition. The acquisition protocol consisted of a macular cube 512 x 128 scan pattern in which a 6.0 x 6.0 mm region of the retina was scanned (a total of 65,536 sampled points) within a scan time of 2.4 seconds and a raster vertical line which passed simultaneously through the PRL, the TZ and the central MA. The precise location and orientation of each scan were determined using the simultaneous OCT grey-scale fundus images. The ellipsoid zone (EZ) band was identified on the OCT scans and classified as: *present* (well defined), *disrupted* (poorly defined or disorganized), or *absent* (complete absence of EZ band). MA was defined on SD-OCT as an abrupt transition from hypo- to hyper-reflective area in the choriocapillaris just under the RPE line. The classification of the EZ band in the region of the PRL was determined by analyzing the vertical line scan that passed through the center of fixation and included the area of BCEA68. In the TZ it was assessed by analyzing the vertical line scan included between the internal border of BCEA68 and the adjacent border of the atrophic area identified by FAF (MA) using the macular cube and the vertical line scans. Each OCT scan was independently evaluated by three different observers (TV, TB and AS). In cases of disagreement among the observers, the opinion of the senior observer (AS) was considered.

Genetic analysis

For the STGD1 patients, all coding exons, including intron-exon boundaries of the *ABCA4* gene (NM_000350) were sequenced. PCR amplification was prepared using the Core System-Robotic Station (Beckman Coulter, USA) using 50 to 100 ng of genomic DNA in 50 mmol/L KCl, 10 mmol/L Tris-HCl, pH 8.3, 5 mmol/L MgCl₂, 200 μmol/L dNTPs, and 0.5

μmol/L for each primer set. AmpliTaq DNA polymerase (1 Unit of AmpliTaq Gold Applied Biosystems Foster City, KA, USA) was added for each 25 μl reaction. PCR was performed by a multiblock MWG PCR System; cycling parameters for the reactions were optimized for each exon: 95°C for 13 min and then 30 cycles of 95°C for 1 min; 64°C for 1 min; 72°C for 51 min (for which 64°C is the primer annealing temperature) with a final extension of 72°C for 10 min. PCR products were purified by the Biomek NX station (Beckman Coulter). PCR products were processed by the Core System-Robotic Station and amplicons were sequenced on the 3730 DNA Analyzer (ABI Foster City, CA). The sequences were assembled and analyzed using SeqScape software ABI Foster City, CA.

Statistical analysis

Univariate and multivariate linear regression were used to investigate correlation between different morphological and functional factors using Stata 13.1 software (StataCorp, College Station, TX).

Results

Fifty-two patients (17 males and 35 females, 36 eyes from the Eye Clinic in Florence and 16 eyes from the Department of Ophthalmology, Columbia University Medical Center, New York) with STGD1 and *ABCA4* mutations were included in the study. The average age was 36.08 ± 13.63 (range 13-69 yrs.). Mean BCVA was 0.84 ± 0.32 logMAR (range 0.1 to 1.3 logMAR). The demographics and clinical findings of the patients are summarized in Table 1 and the genetic characteristic in Table 2.

Morphological and functional features of the PRL

The eccentric PRL was superior to the fovea in 45 eyes (86.5%), nasal in five (9.6%), and temporal in two (3.8%). None of the eccentric PRLs were inferior to the fovea.

Regarding the stability of fixation, the mean BCEA68 value was 9.74 ± 7.39^{o2} (range 0.3 to 27.5) and the mean BCEA99 value was 42.27 ± 35.67^{o2} (range 1.3 to 132.4).

On average, the eccentric PRL was 6.50° ± 2.63 (range 1°-13°) from the fovea (see Fig 1). The mean sensitivity for the 52 PRLs was 10.76 ± 3.70 dB (range from 3.8 to 18.3 dB). In 33 eyes (63.5%) the PRL region was associated with an “intact” EZ band with a mean sensitivity 12.62 ± 2.88 dB. In 19 eyes (36.5%) it was associated with a “disrupted” EZ band and a mean sensitivity of 7.52 ± 2.58 dB. Qualitatively, FAF in the PRL region appeared to be normal in 38 cases (73.1%); 33 of these eyes had intact EZ bands. For the remaining 14 eyes (26.9%) FAF in the PRL region showed an abnormal pattern, either hypoAF or hyperAF.

Table 1 Demographic data of the 52 patients with phenotype, BCVA, PRL, eccentric ellipse area (BCEA) and the presence or not of a transition zone (TZ) with the distance in degrees from the MA

| Patient | Age | Eye | Phenotype | BCVA | PRL | PRL (°) | BCEA 68.2% | TZ (°) |
|---------|-----|-----|-----------|------|------|---------|------------|--------|
| 1 | 27 | OS | 1 | 0.8 | sup | 10 | 12,5 | 7 |
| 2 | 64 | OS | 3 | 1.3 | nas | 7 | 7,8 | no |
| 3 | 45 | OS | 3 | 1.3 | sup | 7 | 5 | no |
| 4 | 43 | OD | 3 | 1.1 | sup | 6 | 6,6 | no |
| 5 | 24 | OD | 2 | 1 | temp | 7 | 14,9 | 6 |
| 6 | 46 | OD | 3 | 1 | sup | 6 | 3,7 | no |
| 7 | 43 | OS | 4 | 0.5 | sup | 1 | 0,3 | no |
| 8 | 39 | OD | 3 | 1.3 | sup | 9 | 24,7 | 6 |
| 9 | 22 | OS | 1 | 0.7 | sup | 4 | 2,6 | 2 |
| 10 | 37 | OS | 4 | 1 | sup | 11 | 14,7 | 9,5 |
| 11 | 39 | OD | 1 | 1 | temp | 6 | 15,2 | no |
| 12 | 29 | OS | 2 | 0.7 | sup | 13 | 10,5 | 11 |
| 13 | 40 | OS | 2 | 1 | sup | 11 | 19,8 | 9 |
| 14 | 36 | OS | 2 | 0.9 | sup | 4 | 8,8 | no |
| 15 | 69 | OD | 3 | 0.9 | sup | 9 | 18,4 | no |
| 16 | 27 | OS | 4 | 1 | sup | 12 | 21,1 | 8 |
| 17 | 46 | OS | 3 | 1 | nas | 7 | 25,5 | 5 |
| 18 | 39 | OS | 1 | 0.7 | sup | 4 | 6,6 | no |
| 19 | 40 | OS | 4 | 1.3 | nas | 5 | 19 | no |
| 20 | 42 | OD | 4 | 1.3 | sup | 10 | 27,5 | 5 |
| 21 | 22 | OD | 1 | 0.9 | sup | 4 | 11,7 | no |
| 22 | 40 | OD | 1 | 0.7 | sup | 5 | 1,8 | 4 |
| 23 | 30 | OS | 2 | 0.7 | nas | 8 | 4,7 | 7 |
| 24 | 19 | OS | 3 | 0.8 | sup | 9 | 10 | 5 |
| 25 | 30 | OD | 3 | 1 | sup | 6 | 18,3 | no |
| 26 | 23 | OS | 2 | 0.8 | sup | 4 | 10,2 | 4 |
| 27 | 32 | OS | 4 | 0.7 | sup | 6 | 4,3 | 4 |
| 28 | 35 | OS | 1 | 0.8 | sup | 5 | 3,9 | 3 |
| 29 | 27 | OD | 1 | 0.8 | sup | 6 | 3,2 | 4 |
| 30 | 49 | OS | 3 | 1.3 | sup | 6 | 15,1 | no |
| 31 | 13 | OS | 3 | 1 | sup | 5 | 1,8 | 3 |
| 32 | 65 | OD | 1 | 1.1 | sup | 6 | 4,7 | no |
| 33 | 21 | OS | 4 | 0.9 | sup | 7 | 3,1 | 4 |
| 34 | 27 | OD | 1 | 0.4 | sup | 8 | 22,8 | 6 |
| 35 | 38 | OD | 1 | 0.7 | sup | 4 | 3,5 | 3 |
| 36 | 23 | OS | 2 | 0.8 | sup | 5 | 6,9 | 2,5 |
| 37 | 33 | OS | 1 | 0.4 | sup | 6 | 4,87 | 2 |
| 38 | 38 | OD | 1 | 1 | sup | 5 | 8,65 | 5 |
| 39 | 31 | OS | 1 | 0.1 | sup | 6 | 8,83 | 5 |
| 40 | 26 | OD | 2 | 1.3 | sup | 7 | 8,92 | 6 |
| 41 | 58 | OS | 2 | 0.6 | sup | 7 | 2,88 | 2 |
| 42 | 47 | OS | 2 | 0.6 | sup | 5 | 5,62 | 3,5 |
| 43 | 26 | OS | 4 | 1 | nas | 9 | 8,5 | 3 |
| 44 | 64 | OD | 1 | 0.9 | sup | 7 | 27,38 | 2 |
| 45 | 34 | OS | 3 | 0.7 | sup | 4 | 2,16 | 1 |
| 46 | 17 | OD | 1 | 1 | sup | 1 | 1,5 | no |
| 47 | 28 | OD | 1 | 1.3 | sup | 7 | 7,98 | 3 |
| 48 | 67 | OD | 3 | 0.3 | sup | 6 | 4,87 | no |
| 49 | 20 | OD | 1 | 0.9 | sup | 1 | 2,93 | no |
| 50 | 17 | OD | 1 | 0.6 | sup | 4 | 6,09 | 2,0 |
| 51 | 46 | OD | 3 | 1 | sup | 10 | 9,52 | 3,5 |
| 52 | 33 | OD | 3 | 1.3 | sup | 10 | 4,46 | 7,5 |

For 17 eyes (32.7%) the eccentric PRL area was located at the edge of the macular atrophy identified by FAF. In 35 of the 52 eyes (67.3%) the eccentric PRL area was 4.59° +/- 2.36 (range 1.5° to 9.5°) away from the edge of MA identified on FAF. A retinal area, located between the PRL and MA, was identified and defined as the TZ. The results are summarized in Table 3.

Using Spearman correlation coefficients, we found that poor BCVA was associated with increased BCEA68 ($r=0.36$,

$p=0.010$) and BCEA99 ($r=0.39$, $p=0.005$) values and decreased PRL sensitivity ($r=-0.42$, $p=0.002$). As expected, BCEA increased with increasing eccentricity ($r=0.54$ and $r=0.51$ for BCEA68 and BCEA99, respectively, $p<0.001$ in both cases). In the PRL area, a disrupted EZ band was associated with poorer BCVA (0.184 logMAR, $p=0.020$) and decreased sensitivity (5 dB, $p<0.001$). Abnormal FAF was correlated with decreased sensitivity (-3 dB, $p=0.002$), but not with BCVA (0.060 logMAR, $p=0.457$).

Table 2 Genetic data of patients

| Patient | allele 1 | allele 2 |
|---------|--|--|
| 1 | c.2791G>A (p.Val931Met) | c.4234C>T (p.Gln1412*) |
| 2 | c.2791G>A (p.Val931Met) | c.3322C>T (p.Arg1108Cys) |
| 3 | c.5417G>A (p.Ser1806Asn) | c.5882G>A (p.Gly1961Glu) |
| 4 | c.5417G>A (p.Ser1806Asn) | c.5882G>A (p.Gly1961Glu) |
| 5 | c.4667+1G>A (p.?) | c.5512C>A (p.His1838Asn) |
| 6 | c.4793C>A (p.Ala1598Asp) | c.4793C>A (p.Ala1598Asp) |
| 7 | c.2461T>A (p.Trp821Arg) | c.5714+5G>A (p.?) |
| 8 | c.634C>T (p.Arg212Cys) | c.3056C>T (p.Thr1019Met) |
| 9 | c.514G>A (p.Gly172Ser) | c.5882G>A (p.Gly1961Glu) |
| 10 | c.982G>T (p.Glu328*) | c.5714+5G>A (p.?) |
| 11 | c.5882G>A (p.Gly1961Glu) | c.6282+1G>C (p.?) |
| 12 | c.3233G>A (p.Gly1078Glu) | c.5882G>A (p.Gly1961Glu) |
| 13 | c.2345G>A (p.Trp782*) | c.6320G>A (p.Arg2107His) |
| 14 | c.203C>T (p.Pro68Leu) | [c.4450C>T (p.Pro1484Ser);c.5882G>A (p.Gly1961Glu)] |
| 15 | c.4297G>A (p.Val1433Ile) | c.4297G>A (p.Val1433Ile) |
| 16 | c.3531C>A (p.Cys1177*) | c.4793C>A (p.Ala1598Asp) |
| 17 | c.247_250dup (p.Ser84Thrfs*16) | c.5087G>A (p.Ser1696Asn) |
| 18 | c.5882G>A (p.Gly1961Glu) | c.3531C>A (p.Cys1177*) |
| 19 | c.4437G>A (p.Trp1479*) | c.6419T>A (p.Leu2140Gln) |
| 20 | c.4437G>A (p.Trp1479*) | c.6419T>A (p.Leu2140Gln) |
| 21 | c.2461T>A (p.Trp821Arg) | c.3323G>A [(p.Arg1108His);c.4297G>A (p.Val1433Ile)] |
| 22 | c.634C>T (p.Arg212Cys) | c.5087G>A (p.Ser1696Asn) |
| 23 | c.768G>T p.=(p.Val256Val) | c.5714+5G>A (p.?) |
| 24 | c.3322C>T (p.Arg1108Cys) | WT |
| 25 | c.3970del (p.Ala1324Argfs*65) | c.5882G>A (p.Gly1961Glu) |
| 26 | c.4383G>C (p.Trp1461*) | c.5929G>A (p.Gly1977Ser) |
| 27 | c.2461T>A (Trp821Arg) | c.5714+5G>A (p.?) |
| 28 | c.3933G>A (p.Gly978Asp) | c.5882G>A (p.Gly1961Glu) |
| 29 | c.2519T>G (p.Met840Arg) | c.5882G>A (p.Gly1961Glu) |
| 30 | c.1245C>A (p.Asn415Lys) | c.5882G>A (p.Gly1961Glu) |
| 31 | c.343_381delinsGGACAA (p.Asn115_Thr127delinsGlyGln) | p.[c.1622T>C (p.Leu541Pro);c.3113C>T (p.Ala1038Val)] |
| 32 | c.571-2A>T (p.?) | c.5882G>A (p.Gly1961Glu) |
| 33 | c.5018+2T>C (p.?) | c.5898+5del (p.?) |
| 34 | c.6537del (p.Pro2180Leufs*3) | WT |
| 35 | c.3531C>A (p.Cys1177*) | c.5882G>A (p.Gly1961Glu) |
| 36 | c.634C>T (p.Arg212Cys) | c.3056C>T (p.Thr1019Met) |
| 37 | c.5882G>A (p.Gly1961Glu) | c.2382+1G>A (p.?) |
| 38 | c.6320G>A (p.Arg2107His) | c.3523-1G>A (p.?) |
| 39 | c.5882G>A (p.Gly1961Glu) | c.6229C>T (p.Arg2077Trp) |
| 40 | c.4139C>T (p.Pro1380Leu) | c.4139C>T (p.Pro1380Leu) |
| 41 | c.4139C>T (p.Pro1380Leu) | c.5087G>A (p.Ser1696Asn) |
| 42 | c.318T>G (p.Tyr106*) | c.2588G>C (p.Gly863Ala) |
| 43 | c.2552G>A (p.Gly851Asp) | c.6079C>T (p.Leu2027Phe) |
| 44 | c.5882G>A (p.Gly1961Glu) | c.5882G>A (p.Gly1961Glu) |
| 45 | c.5882G>A (p.Gly1961Glu) | c.5882G>A (p.Gly1961Glu) |
| 46 | p.[c.1622T>C (p.Leu541Pro);c.3113C>T (p.Ala1038Val)] | c.5882G>A (p.Gly1961Glu) |
| 47 | c.5882G>A (p.Gly1961Glu) | c.6005+1G>T (p.?) |
| 48 | c.5882G>A (p.Gly1961Glu) | c.5882G>A (p.Gly1961Glu) |
| 49 | c.1622T>C (p.Leu541Pro) | c.5882G>A (p.Gly1961Glu) |
| 50 | c.1622T>C (p.Leu541Pro) | c.5882G>A (p.Gly1961Glu) |
| 51 | p.[c.1622T>C (p.Leu541Pro);c.3113C>T (p.Ala1038Val)] | |
| 52 | c.5882G>A (p.Gly1961Glu) | c.2160+584A>G (p.?) |

Morphological and functional features of TZ

Of the 35 eyes with a TZ, this was associated with an “intact” EZ band in eight eyes, with a “disrupted” EZ band in 16 eyes, and with “absence” of the EZ band in 11 eyes. Mean retinal sensitivity

within the TZ was significantly decreased (mean value 5.92 +/- 4.69 dB) compared to sensitivity in the PRL area ($p < 0.05$). Specifically, in eyes with intact EZ bands we found a mean sensitivity of 11.03 +/- 4.65 dB, compared to 6.31 +/- 3.41 dB when the EZ band was disrupted, and 1.65 +/- 1.79 dB when it was absent

Table 3 Mean values of BCEA, BCVA and Visual Sensitivity in the two different groups of fixation. MA= Macular Atrophy

| | Fixation at the edge of MA (17/52 eyes) | Fixation far from the edge of MA (35/52 eyes) |
|----------------------|---|---|
| Eccentricity from MA | None | 4.67 +/- 2.38° |
| Fixation (BCEA68) | 8.85 +/- 6.22°2 | 10.17 +/- 7.95°2 |
| Visual Acuity (BCVA) | 0.97 +/- 0.28 logMAR | 0.85 +/- 0.27 logMar |
| Visual Sensitivity | 9.54 +/- 3.26dB | 11.35 +/- 3.80dB |

(Fig. 6). With the exception of four eyes the FAF pattern in the TZ was abnormal; it was either hyper- or hypo-autofluorescent. In addition flecks were observed in the TZ in 15 of these eyes and they extended from the RPE and through the EZ band (see Fig. 5c). Results are shown in Table 3 and Table 4.

We also analysed data categorizing patients into the four phenotype sub-groups based on fundus appearance and interestingly we found that stage 1 patients had better sensitivity (13.34 +/- 2.52 db) and better stability of fixation (8.05 +/- 6.07°2) that those in stage 2 (respectively, 11.07 +/- 3.06 db and 10.83 +/- 5.08°2) stage 3 (9.28 +/- 2.80 db and 12.45 +/- 8.19°2) or stage 4 (6.98 +/- 3.37 db and 12.86 +/- 9.86°2).

Discussion

In this study a multimodal analysis of the PRL and the TZ areas has been performed in a group of STGD1 patients. Our results show that, for the majority of eyes, the eccentric PRL was associated with relatively preserved visual sensitivity, the presence of an intact EZ band and qualitatively normal FAF. In addition, it was located outside the border of central MA as previously reported by other authors [8–10]. In these cases we observed a TZ between the PRL and the central atrophic area; this area was associated with morphological and functional abnormalities that extended beyond the limit of the dark atrophic lesion identified by FAF imaging. This is in agreement with previous findings [17, 19] in STGD and suggests the presence of subclinical alterations affecting apparently non-atrophic retinal areas. In a previous study Reinhard et al. [20] found a weak correlation between the eccentricity of the PRL and fixation stability: the

Table 4 OCT, SW-FAF and MP-1 values in the PRL and in the TZ (when present)

| | PRL area (52/52 eyes) | TZ area (35/52 eyes) |
|--------------------|-----------------------|----------------------|
| EZ present | 33(63.5%) | 8(15.6%) |
| EZ disrupted | 19(36.5%) | 16(50%) |
| EZ absent | 0 | 11(34.4%) |
| FAF normal | 38(73.1%) | 4(11.4%) |
| FAF abnormal | 14(26.9%) | 31(88.6%) |
| Visual Sensitivity | 10.76 +/- 3.70 dB | 5.92 +/- 4.69 dB |

Bolded data are the most important findings

eccentricity of PRL was correlated with more unstable fixation. In addition visual acuity showed a statistically significant positive correlation with the fixation locus.

In our investigation we found that PRLs located outside the border of the MA, although exhibiting more unstable fixation, were associated with better BCVAs and visual sensitivity values than PRLs located at the border of the MA. The latter, despite being associated with more stable fixation, had decreased BCVAs and visual sensitivity values. The implications of these findings are that for STGD1 patients a PRL outside the border of the atrophic central area would result in improved visual function. This is in contrast to reports of the PRL being located closer to the central atrophic area in AMD patients [11]. One possible explanation for this difference between the two diseases is the age of the patients. STGD1 patients are generally younger than AMD patients, the visual system may have greater plasticity, and through experience the patients may learn to use a relatively healthier retinal area as their PRL. Moreover disease progression is slower and is usually symmetric in both eyes. The existence of multiple PRLs has also been investigated in the past and some authors concluded that they might be an expression of an unstable transitional stage of patients who developed macular disease recently as in AMD. For most STGD patients, keeping several PRL seems to be an unfavorable strategy to solve one task [20]. In our study we did not find any patient with more than one PRL.

We also investigated the correlation between EZ band integrity, visual sensitivity and FAF in the PRL area and in the TZ to better clarify the physiopathology of retinal degeneration in STGD1. We already know that RPE atrophy in the macula is characteristic of this disease; it is commonly assumed that in STGD1 there is an accumulation of lipofuscin within the RPE leading to RPE loss and to a degeneration of the photoreceptors [4] but there is controversy as to whether photoreceptor loss/dysfunction occurs before or after the RPE is affected; investigators have questioned whether RPE atrophy precedes or follows photoreceptor cell loss in STGD1 [19, 21–24].

Based on a comparison of SD-OCT and FAF results, Gomes et al. [19] hypothesized that photoreceptor loss occurred before RPE loss. The authors suggested that photoreceptors may be affected earlier than RPE atrophic changes as detected by short wavelength FAF, as the measurement of the

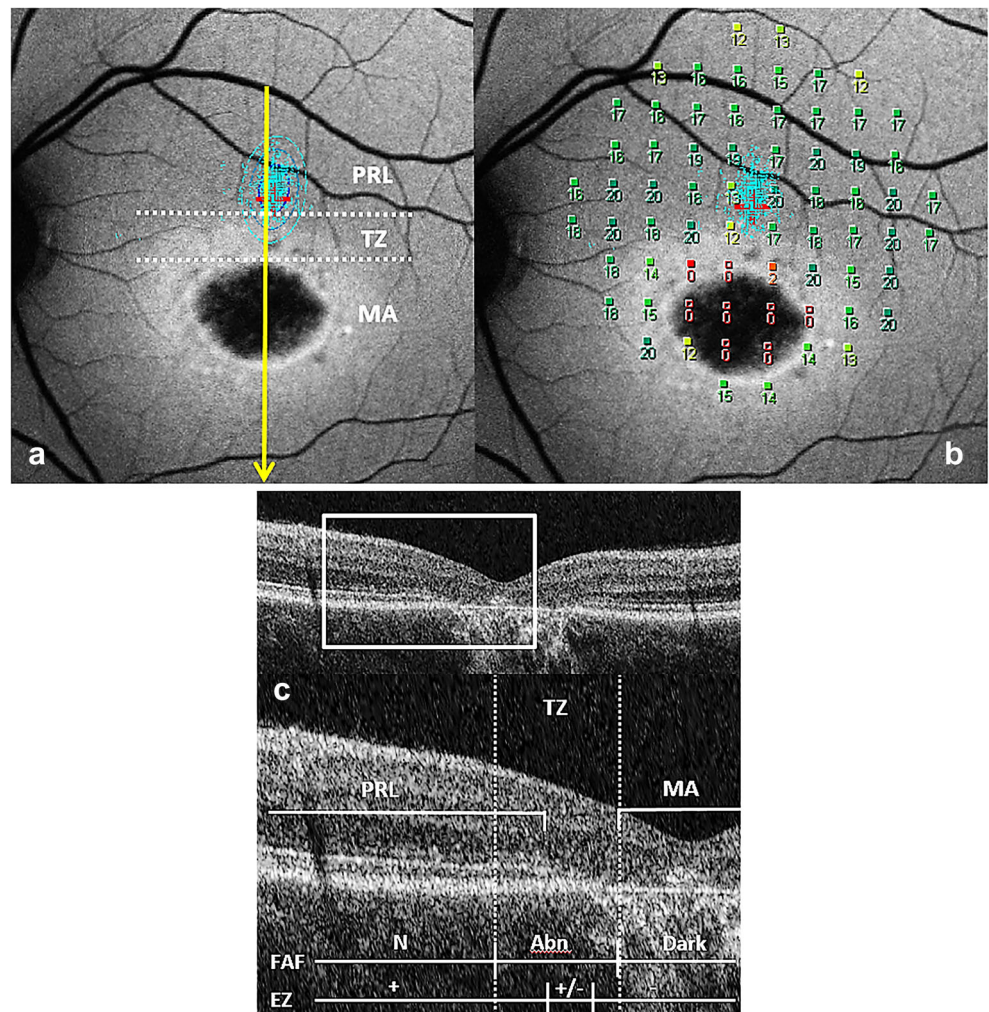
diameter of hypoautofluorescent area on FAF was less than the extent of the EZ loss observed on SD-OCT. Our multi-modal analysis showing the presence of structural and functional abnormalities, e.g., disruption of the EZ band, decreased visual sensitivity and altered FAF affecting apparently non-atrophic retinal areas, is in agreement with the above hypothesis.

It has also been suggested that, in the mildest cases of STGD1, results were consistent with changes in the photoreceptor layer occurring simultaneously with the development of abnormalities in the RPE layer. This hypothesis is based on a recent study [25] that compared structural changes observed with polarization-sensitive OCT to those visible on short wavelength (SW) FAF. Nevertheless, a contribution to SW-FAF from degenerating photoreceptor cells in the advancing front of atrophy could explain why the size of the area of hypoautofluorescence (atrophy) can be underestimated in SW-FAF as compared to NIR-FAF images and why the diameter of the area of absent SW-FAF inadequately reflects the spatial extent of photoreceptor cell abnormalities visualized in SD-OCT images.

Lastly, in a recent study by Sparrow et al. [7] that evaluated retinal flecks on SW and NIR-FAF, the authors indicated that the "bright" SW-FAF signal from flecks likely originates from augmented lipofuscin formation in degenerating photoreceptor cells impaired by the failure of RPE confirming that RPE alterations precede photoreceptor cell degeneration in STGD1.

In our study the sequence and nature of structural changes observed spatially across the TZ at one specific time (time of OCT acquisition) suggests a specific pattern of progression of the disease. However, the reader should be reminded that this is based on observations on different retinas (from different patients) at one time point; ideally the proposed pattern of progression should be based on a prospective analysis of retinal changes over-time. We suggest that, initially, the accumulation of toxic metabolites causes RPE dysfunction that is associated with surviving photoreceptors. At this stage FAF is abnormal (RPE altered but still functioning) visual sensitivity is relatively good and there is preservation of the EZ band (Figs. 2, 3, 4 and 5). The location of the eccentric PRL may be associated with this area. This stage is followed by photoreceptor damage; further changes in FAF, loss

Fig. 3 Patient n.28



and/or disruption of the EZ band (i.e., loss of photoreceptors), and decreased visual sensitivity. PRLs are rarely associated with this area. Finally, in the last stages of the disease, RPE cell death occurs: there is “hypoAF”, the EZ band is absent and sensitivity non-recordable. This stage is represented by central MA (Fig. 6).

Through this multimodal analysis, the results of our study suggest that RPE changes appear to be the primary event leading to photoreceptor degeneration and then to RPE loss. The proposed sequence of structural and functional changes presented above provides a possible model for disease progression, and could aid in determining the potential efficacy of new therapies. In fact, gene therapy could be helpful in preserving retina in the first stages of the degenerative process when RPE dysfunction occurs but photoreceptors are still present. Other strategies such as “stem cells” or “retinal transplantation” could be helpful in restoring visual function in retinal areas at a more advanced stage of the disease process.

An intact EZ band is an important indicator of rod and cone function and in our study we have related the appearance and integrity of the EZ band on SD-OCT directly to localized measures of visual function obtained with the MP-1. Our study confirms that SD-OCT provides more information regarding the stage and nature of the disease process than FAF analysis in STGD, as previously found [22, 26]: even when FAF appears to be altered, the presence of an intact EZ band can be used to differentiate between an area that would respond better to gene therapy from one that would not be amenable to treatment.

Our study has some limitations: it is a retrospective cross-sectional study, not a prospective longitudinal study: it is based on observations on different retinas (from different patients) at one time point. Moreover, we did not include NIR-FAF imaging. Lastly, it is also possible that different phenotypic subtypes of STGD1 based on full-field ERG results may have influenced our results. As we had limited full-field ERG

Fig. 4 Patient n.25

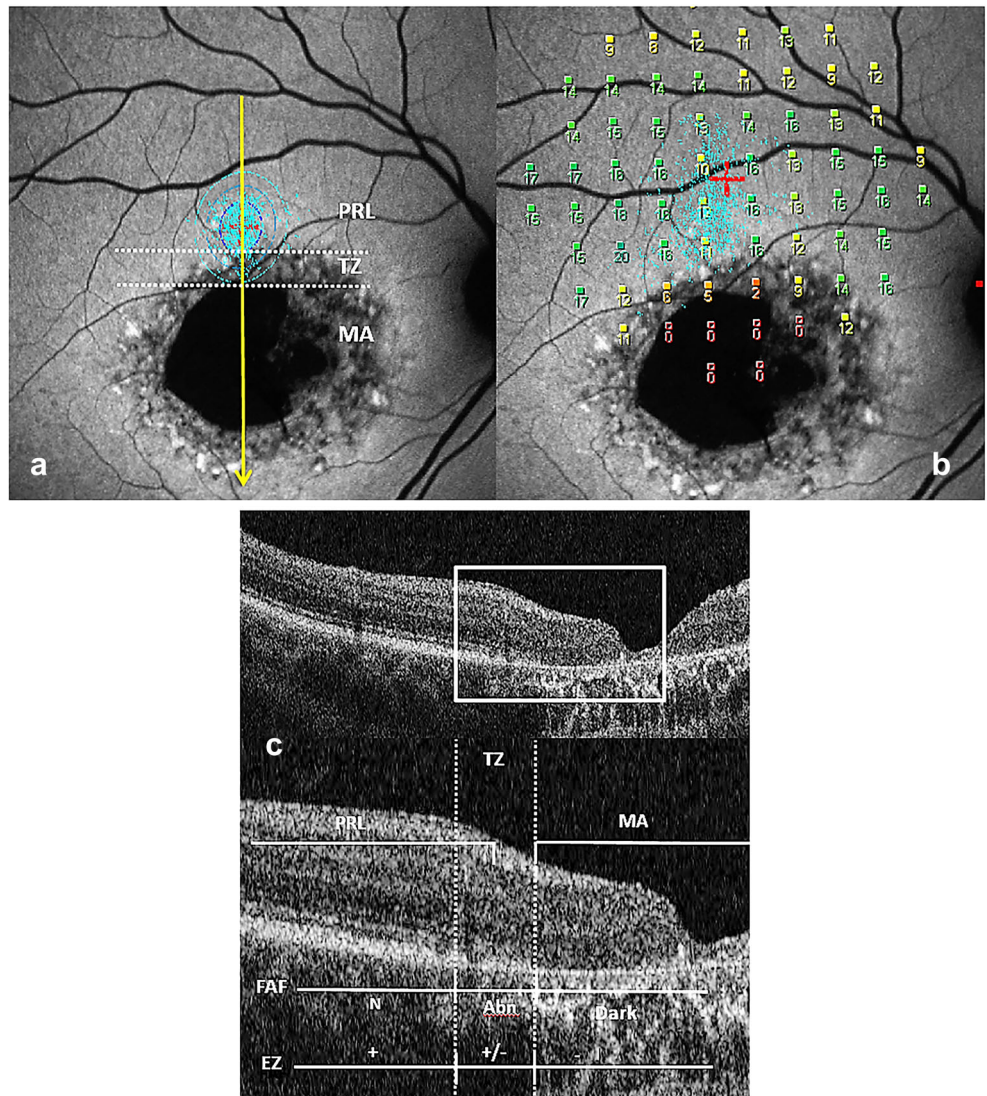
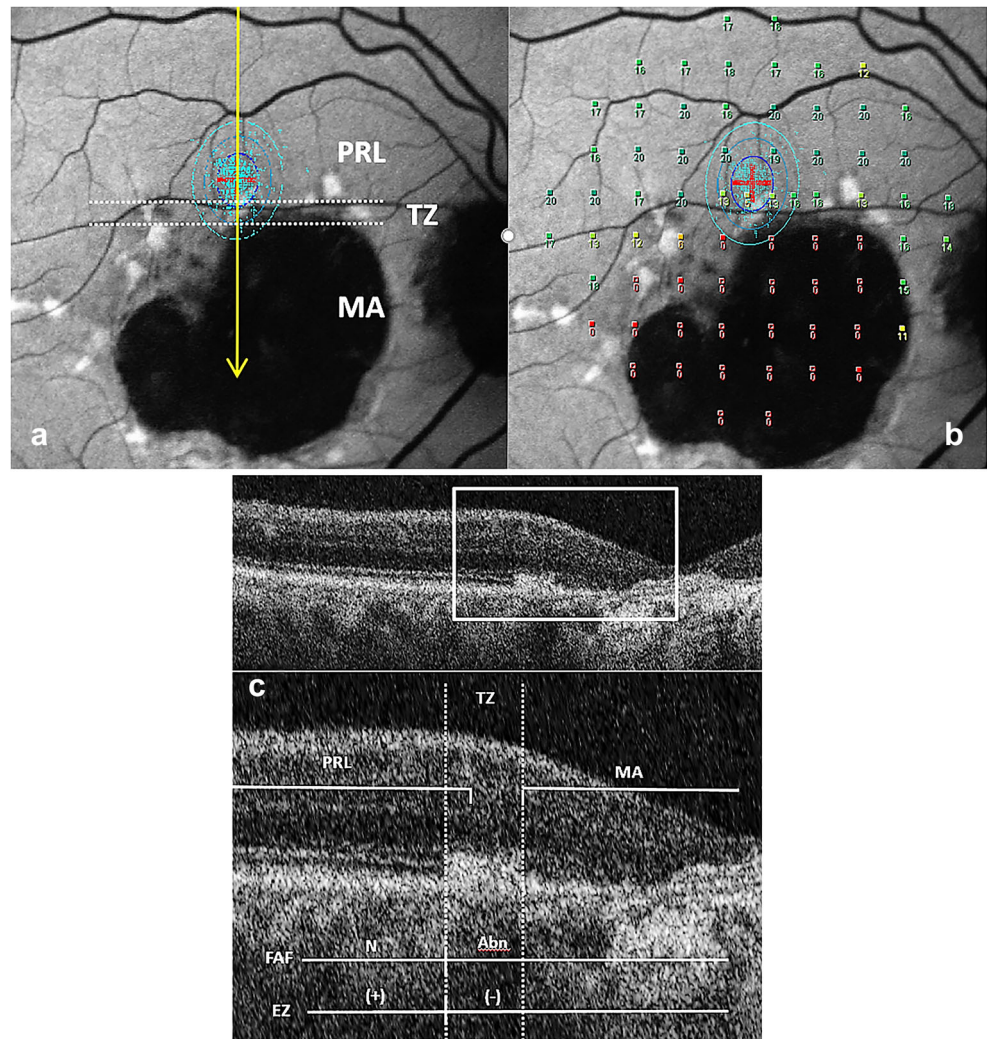


Fig. 5 Patient n.32 with PRL near to the MA with a retinal fleck in the TZ



data on our patients, we could not classify them based on the three phenotypic groups proposed by Lois et al. [27], so we cannot draw any conclusions regarding the influence of these three phenotypic subtypes on our results.

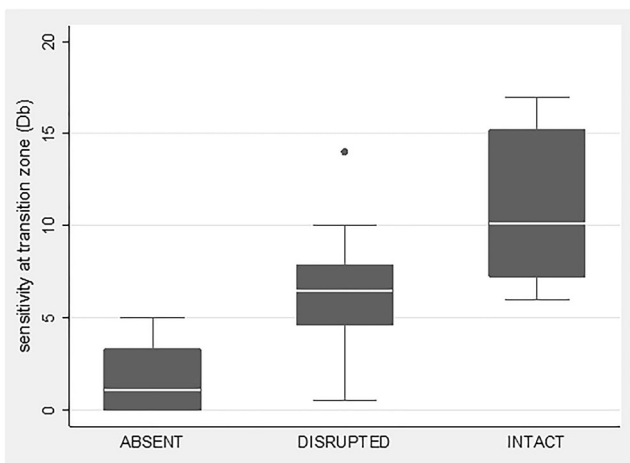


Fig. 6 Visual sensitivity at transition zone compared to integrity of the EZ band

In conclusion, in STGD1 patients the PRLs are located in “healthier” retinal areas, away from the border of MA and are associated with relatively good visual sensitivity, a preserved EZ band and qualitatively normal or slightly altered FAF. The TZ, when present, shows an abnormal FAF pattern associated with changes in the EZ band and decreased visual sensitivity. Morphological and functional retinal abnormalities extend beyond the limits of the atrophic lesion identified by FAF; the area of EZ band loss is more extensive than that of RPE atrophy identified by the hypoAF pattern. Thus, our study hypothesizes a sequence of retinal and functional changes with disease progression that may help in the planning of future therapies. RPE dysfunction seems to be the primary event that leads to a photoreceptors loss and then to RPE loss.

A correlation of functional and structural (MP-1, SD-OCT, FAF) data may help clarify the physiopathological mechanisms underlying STGD1 and improve the management of this disease. Further studies are needed to clarify and define the role of multimodal imaging for monitoring the progression of the disease and its response to future therapeutic interventions.

Compliance with ethical standards

Funding The National Eye Institute/NIH EY09076, Foundation Fighting Blindness and Research to Prevent Blindness of the Department of Ophthalmology, Columbia University provided financial support in the form of grants. S.H.T., a member of the RD-CURE Consortium, is supported by the Tistou and Charlotte Kerstan Foundation, the Schneeweiss Stem Cell Fund, New York State [C029572], the Foundation Fighting Blindness New York Regional Research Center Grant [C-NY05-0705-0312], and the Joel Hoffman Fund. The sponsors had no role in the design or conduct of this research.

Conflict of interest All authors certify that they have no affiliations with or involvement in any organization or entity with any financial interest (such as honoraria; educational grants; participation in speakers' bureaus; membership, employment, consultancies, stock ownership, or other equity interest; and expert testimony or patent-licensing arrangements), or non-financial interest (such as personal or professional relationships, affiliations, knowledge or beliefs) in the subject matter or materials discussed in this manuscript.

Ethical approval All procedures performed in studies involving human participants were in accordance with the ethical standards of the institutional and/or national research committee and with the 1964 Helsinki Declaration and its later amendments or comparable ethical standards. For this type of study formal consent is not required.

References

1. Fishman GA (1976) Fundus flavimaculatus: a clinical classification. *Arch Ophthalmol* 94:2061–2067
2. Gass JDM (1997) Heredodystrophic Disorders Affecting the Pigment Epithelium and Retina. In: Gass JDM. *Stereoscopic Atlas of Macular Disease. Diagnosis and Treatment*. Mosby, St.Louis-London-Philadelphia-Sidney-Toronto:p.303-435.
3. Rozet JM, Gerber S, Ducroq D, Hamel C, Dufier JL, Kaplan J (2005) Les dystrophies maculaires héréditaires. *J Fr Ophtalmol* 28(1):113–124
4. Glazer LC, Dryja TP (2002) Understanding the etiology of Stargardt's disease. *Ophth Clin North Am* 15(1):93–100
5. Walia S, Fishman GA (2009) Natural History of Phenotypic Changes in Stargardt Macular Dystrophy. *Ophthalmic Genetics* 30:63–68
6. Eagle RC Jr, Lucier AC, Bernardino VB Jr, Yanoff M (1980) Retinal pigment epithelial abnormalities in fundus flavimaculatus: a light and electron microscopic study. *Ophthalmology*. 87(12): 1189–1200
7. Sparrow JR, Marsiglia M, Allikmets R, Tsang SH, Lee W, Duncker T, Zernant J (2015) Flecks in Recessive Stargardt Disease: Short-Wavelength Autofluorescence, Near-Infrared Autofluorescence, and Optical Coherence Tomography. *Invest Ophthalmol Vis. Sci.* 56:5029–5039
8. Sunness JS, Applegate CA, Haselwood D, Rubin GS (1996) Fixation Patterns and Reading Rates in Eyes with Central Scotomas from Advanced Atrophic Age-related Macular Degeneration and Stargardt Disease. *Ophthalmology* 103:1458–1466
9. Messias A, Reinhard J, Velascoe Cruz AA, Dietz K, MacKeben M, Trauzettel-Klosinski S (2007) Eccentric fixation in Stargardt's disease assessed by Tubingen perimetry. *Invest Ophthalmol Vis Sci.* 48(12):5815–5822
10. Greenstein VC, Santos RAV, Tsang SH, Smith RT, Barile GR, Seiple W (2008) Preferred Retinal Locus in Macular Disease: Characteristics and Clinical Implications. *Retina* 28(9):1234–1240
11. Cheung SH, Legge GE (2005) Fuctional and cortical adaptations to central vision loss. *Visual Neuroscience* 22:187–201
12. Huxlin KR (2008) Perceptual plasticity in damaged adult visual systems. *Vision Research* 48:2154–2166
13. Tarita-Nistor L, Gonzalez EG, Markowitz SN, Steinbach MJ (2009) Plasticity of fixation in patients with central vision loss. *Visual Neuroscience* 26:487–494
14. Macedo AF, Cardoso Nascimento SM, Silva Gomes AO, Teixeira Puga A (2007) Fixation in patients with juvenile macular disease. *Optometry and Vision Science* 84(9):852–858
15. Schuchard RA (2005) Preferred retinal loci and macular scotoma characteristics in patients with age-related macular degeneration. *Canadian Journal of Ophthalmology* 40:303–312
16. Lazow MA, Hood DC, Ramachandran R, Burke TR et al (2011) Transition Zones Between Healthy and Diseased Retina in Choideremia (CHM) and Stargardt Disease (STGD) as Compared to Retinitis Pigmentosa (RP). *Invest Ophthalmol Vis Sci* 52(13): 9581–9590
17. Fishman GA, Stone EM, Grover S et al (1999) Variation of clinical expression in patients with Stargardt dystrophy and sequence variations in the ABCR gene. *Arch Ophthalmol.* 17(4):504–510
18. Crossland MD, Dunbar HMP, Rubin GS (2009) Fixation stability measurement with MP1microperimeter. *Retina.* 29:651–656
19. Gomez NL, Greenstein VC, Carlson AN, Tsang SH, Smith RT, Carr RE, Hood DC, Chang S (2009) A comparison of Fundus Autofluorescence and Retinal Structure in Patients with Stargardt Disease. *Invest Ophthalmol Vis Sci.* 50:3953–3959
20. Reinhard J, Messias A, Dietz K et al (2007) Quantifying fixation in patients with Stargardt disease. *Vision Res* 47(15):2076–2085
21. Testa F, Rossi S, Sodi A, Passerini I, Di Iorio V, Della Corte M, Banfi S, Surace EM, Menchini U, Auricchio A, Simonelli F (2012) Correlation between photoreceptor layer integrity and visual function in patients with Stargardt disease: implications for gene therapy. *Invest Ophthalmol Vis Sci* 53(8):4409–4415
22. Ergun E, Hermann B, Wirtitsch M, Unterhuber A, Ko TH et al (2005) Assessment of central visual function in Stargardt's disease/fundus flavimaculatus with ultrahigh-resolution optical coherence tomography. *Invest Ophthalmol Vis Sci.* 46(1):310–316
23. Testa F, Melillo P, Di Iorio V et al (2014) Macular Function and Morphologic features in Juvenile Stargardt Disease. *Ophthalmol* 121:2399–2405
24. Burke TR, Duncker T, Woods RL et al (2014) Quantitative fundus autofluorescence in recessive stargardt disease. *Invest Ophthalmol Vis Sci.* 55:2841–2852
25. Ritter M, Zotter S, Schmidt WM et al (2013) Characterization of Stargardt disease using polarization-sensitive optical coherence tomography and fundus autofluorescence imaging. *Invest Ophthalmol Vis Sci.* 54:6416–6425
26. Greenstein VC, Schuman AD, Lee W et al (2015) Near-infrared autofluorescence: its relationship to short-wavelength autofluorescence and optical coherence tomography in recessive stargardt disease. *Invest Ophthalmol Vis Sci.* 56(5):3226–3234
27. Lois N, Holder GE, Bunce C et al (2001) Phenotypic subtypes of Stargardt macular dystrophy-fundus flavimaculatus. *Arch Ophthalmol.* 119(3):359–369